

NASICON-PEO (Polyethylene Oxide) Polymer-in-Ceramic Composite Electrolytes: Thermal, Structural and Electrical Properties

N. Yusri¹, N. A. Malim¹, S. Rudhzhiah², N. A. Dzulkurnain³ and N. A. Mustaffa^{1,*}

¹Faculty of Applied Sciences, Universiti Teknologi MARA, Shah Alam Selangor 40450, Malaysia

²Centre of Foundation Studies, Universiti Teknologi MARA, Cawangan Selangor, Kampus Dengkil, Selangor 43900, Malaysia

³International Battery Center Sdn. Bhd., HEBATT, Lot-G4, HIVE 8 Taman Teknologi, Kuala Lumpur 57000, Malaysia

(*Corresponding author's e-mail: nuramalina@uitm.edu.my)

Received: 31 December 2024, Revised: 7 February 2025, Accepted: 14 February 2025, Published: 1 May 2025

Abstract

A composite electrolyte consisting of sodium super ionic conductor (NASICON) $\text{LiSn}_2\text{P}_3\text{O}_{12}$ (LSPO) and a polymer electrolyte (80:20 polyethylene oxide (PEO) with LiTFSI salt) was prepared using the solution casting method. The thermal stability of the composite was assessed, revealing a second-stage decomposition temperature range between 375 and 462 °C, with a glass transition temperature (T_g) of 28 °C. X-ray diffraction (XRD) analysis indicated low crystallinity in PEO-LiTFSI, with no significant structural changes, despite the emergence of a new peak at 20.7 °C. Electrochemical impedance spectroscopy (EIS) was used to investigate the electrical properties at seven different temperatures (30, 40, 50, 60, 70, 80 and 90 °C), with the highest bulk conductivity of 6.2825×10^{-5} S/cm observed at 50 °C. The results demonstrate that the addition of LSPO ceramic electrolyte and temperature significantly influence the thermal, structural, and electrical properties of the composite electrolyte.

Keywords: Composite electrolyte, NASICON (LSPO), Polymer electrolyte, PEO-LiTFSI electrochemical impedance spectroscopy (EIS), Thermal stability, Bulk conductivity

Introduction

Secondary lithium-ion batteries are widely used for their high output voltage and energy density, making them essential in modern energy storage systems. However, the use of liquid electrolytes in these batteries, which consist of lithium salts dissolved in organic solvents, raises significant safety concerns due to their flammability, particularly in large-capacity applications [1]. The low boiling points of organic liquid electrolytes pose risks of leakage and explosions, limiting the scalability and safety of current lithium-ion batteries [2]. Furthermore, the use of metal anodes to improve energy density is hindered by the uncontrolled formation of dead lithium, reducing battery performance and lifespan.

These challenges underscore the urgent need for the development of solid-state batteries, which use solid electrolytes to address the safety and performance limitations of liquid electrolytes. Recent research has focused on composite polymer electrolytes (CPEs), which combine ceramic and polymer materials to harness the advantages of both. A promising approach, “polymer-in-ceramic” composite electrolytes, integrates ceramic as the primary component, offering excellent mechanical, thermal, and electrochemical stability [3]. Ceramic electrolytes typically show high ionic conductivity and a wide electrochemical stability window at ambient temperatures. However, their widespread application is limited by issues such as poor interfacial contact with electrodes and high interfacial resistance at the grain boundaries, which reduce their overall performance [3].

In contrast, solid polymer electrolytes (SPEs) offer superior flexibility and better electrode contact, but they suffer from low ionic conductivity, ranging from 10 to 10^{-8} S/cm at room temperature. This limitation leads to increased internal polarization, reducing energy efficiency and charging capacity, which limits the applicability of SPEs in high-performance batteries [4].

Composite electrolytes (CEs), which combine the benefits of both polymer and ceramic electrolytes, present a promising solution to improve the performance of solid-state batteries. Despite this potential, the research on composite electrolytes is still limited, and further exploration is necessary to optimize their properties and performance [1].

This study aims to bridge the gap in solid-state battery research by systematically investigating PEO-LiTFSI composites with varying LSPO content, focusing on their thermal, structural, and electrochemical characteristics. Understanding these properties is essential for advancing solid-state battery technology and mitigating safety concerns, such as overheating, overcharging, and short-circuiting in lithium-ion batteries. By integrating polymer electrolytes into ceramic systems, this research seeks to enhance the electrical properties of composite materials, paving the way for more reliable and high-performance battery technologies.

Beyond technical advancements, this study holds significant societal and industrial relevance, aligning with global trends in renewable energy, electric vehicles (EVs), and sustainable technology. The development of solid-state batteries, such as NASICON-PEO composites, addresses the urgent need for safer and more efficient energy storage solutions. In renewable energy applications, these batteries can enhance large-scale storage systems, supporting grid stability and accelerating clean energy adoption. In the EV industry, they offer improved safety, energy density, and lifespan, extending vehicle range while reducing environmental impact. By contributing to the advancement of solid-state battery technology, this research supports global sustainability goals, facilitating the transition toward cleaner energy solutions and a more sustainable, circular economy.

Materials and methods

In this study, the composite electrolyte system incorporates NASICON (Sodium Super Ionic Conductor) and PEO (Polyethylene Oxide) due to their complementary and unique properties, which make them highly suitable for enhancing the performance of solid-state batteries [1,10,11]. NASICON is known for its high ionic conductivity and exceptional stability, both thermally and electrochemically [9]. Its structure, characterized by a three-dimensional framework, allows for rapid ion transport, making it an ideal candidate for high-performance solid-state electrolytes [9,12]. NASICON-based materials have been widely studied for their ability to conduct lithium ions at ambient temperatures, and their stability at high voltages and temperatures makes them particularly promising for applications in energy storage devices [1,9]. This high ionic conductivity is essential for the development of efficient solid-state electrolytes, which can address the limitations of traditional liquid electrolytes [2,10].

On the other hand, PEO offers flexibility and excellent compatibility with electrodes, making it a highly attractive component for composite electrolytes [10,12]. As a polymer, PEO provides mechanical flexibility, which is critical for the fabrication of safe, durable solid-state batteries [10,12]. Additionally, PEO's ability to form stable complexes with lithium salts, such as LiTFSI, enhances its ionic conductivity, although it is limited by its relatively low intrinsic conductivity [4,10]. By integrating PEO with NASICON, the resulting composite electrolyte benefits from the high ionic conductivity and structural stability of NASICON, while also maintaining the flexibility and compatibility of PEO, making the system more suitable for practical battery applications [10,11]. Together, NASICON and PEO complement each other in the composite electrolyte, balancing the need for both high ionic conductivity and the flexibility required for efficient, long-lasting solid-state batteries [1,10,11]. This combination makes NASICON-PEO composites a promising candidate for enhancing the performance of next-generation energy storage devices [10,11].

Ceramic electrolytes (LSPO) were prepared using the sol-gel method as previously reported in the literature [9]. A molar ratio of 1:2:3 was used for lithium acetate (CH_3COOLi), stannum (IV) chloride pentahydrate ($\text{SnCl}_4 \cdot 5\text{H}_2\text{O}$), and ammonium phosphate

($\text{H}_{12}\text{N}_3\text{O}_4\text{P}$), which were dissolved under magnetic stirring. Citric acid ($\text{C}_6\text{H}_8\text{O}_7$), polyethylene glycol ($\text{C}_2\text{H}_6\text{O}_2$), and ammonium hydroxide (NH_4OH) were then added and stirred homogeneously into the solution for 24 h. The resulting solution was vaporized at $80\text{ }^\circ\text{C}$ for 4 h, producing a gel. This gel was dried in an oven at $150\text{ }^\circ\text{C}$ for another 24 h.

The dried precursor powder was ground for 30 min using a mortar and pestle to achieve a fine, uniform powder. The grinding process aimed to reduce particle size and enhance homogeneity before the thermal treatment. The powder was then subjected to a firing process at 500 , 550 , 600 and $650\text{ }^\circ\text{C}$ for 24 h in a controlled furnace atmosphere. After each firing step, the sample was allowed to cool to room temperature and was re-ground for another 30 min to ensure the production of a fine, uniform powder. This repeated

grinding process helped achieve consistent particle size distribution across the samples, essential for further structural and electrical characterization.

Polymer electrolytes (PE) were prepared using 80 wt% polyethylene oxide (PEO) and 20 wt% lithium bis(trifluoromethane)sulfonimide (LiTFSI) via a casting technique. These materials were used as received. For the composite electrolytes (CE), 80 wt% LSPO ceramic electrolytes and 20 wt% polymer electrolytes were mixed using the solution casting technique. The components were dissolved in anhydrous acetonitrile and stirred at $60\text{ }^\circ\text{C}$ for 12 h. The resulting solution was cast onto a petri dish and placed under vacuum at $45\text{ }^\circ\text{C}$ for 5 h to evaporate the solvent. Finally, the composite membrane was peeled off the dish and used for further characterizations.

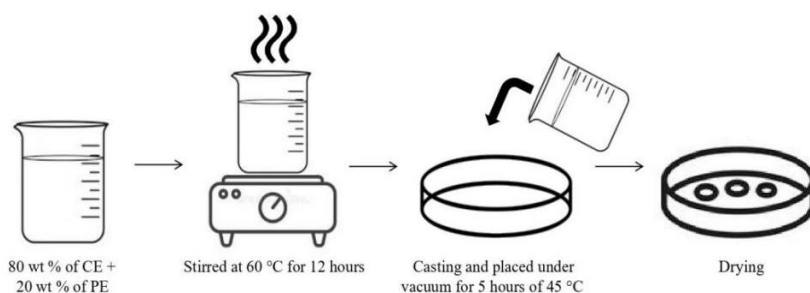


Figure 1 Methods of preparing the composite electrolytes system.



Figure 2 The composite electrolytes sample.

The thermal stability of the composite electrolytes was analyzed using a thermogravimetric analyzer (TGA). Approximately 10 mg of the sample was loaded into a crucible and placed in the center of the heating chamber. TGA scans were conducted at a constant heating rate of $10\text{ }^\circ\text{C}/\text{min}$ over a temperature range of 0 to $1,200\text{ }^\circ\text{C}$.

Differential scanning calorimetry (DSC) was used to measure the glass transition temperatures of the

electrolytes. DSC measurements were recorded over a temperature range of 0 to $100\text{ }^\circ\text{C}$, with a heating rate of $10\text{ }^\circ\text{C}/\text{min}$ and a cooling rate of $5\text{ }^\circ\text{C}/\text{min}$. The DSC curve for the composite was recorded during a heating scan in the temperature range of 0 to $95\text{ }^\circ\text{C}$.

X-ray diffraction (XRD) was used to determine the structural properties of the composite electrolyte samples using PANalytical-X'pert³ with $\text{CuK}\alpha$ radiation

source at room temperature. Measurements were taken with a 2θ range from 10 to 40 ° at a step size of 0.026 °. Electrochemical impedance spectroscopy (EIS) was conducted to measure the total ionic conductivity of the composite sample and to determine its bulk conductivity at various temperatures. Impedance plots were recorded for the composite sample at temperatures ranging from 30, 40, 50, 60, 70, 80 and 90 °C. The bulk conductivity (σ_b) representing the ionic conductivity of the samples was calculated using the relation $\sigma_b = d/(A \times R_b)$, where d represents the sample thickness, A is the cross-sectional area of the sample ($A = \pi r^2$), and R_b is the bulk resistance. The average thickness of the pellets was 0.21 cm, and A was calculated to be 0.14 cm².

Results and discussion

TGA was used to determine the thermal properties of the composite system. As shown in **Figure 3**, the TGA results revealed a multi-stage decomposition process. The initial weight loss (Δm_1) of 0.68 % below 200 °C is attributed to the removal of absorbed water and excess solvent, consistent with previous findings on polymer-in-ceramic electrolytes [3,9]. The second stage (Δm_2), occurring between 200 and 375 °C, resulted in a gradual weight loss of 35.56 %, primarily due to the decomposition of polymer electrolyte components. The final weight loss stage (Δm_3) before reaching a thermal plateau at 462 °C exhibited an additional 6.39 % weight loss, further confirming the breakdown of the polymer matrix [3].

The observed decomposition behavior aligns with prior research, which reports that the initial weight loss below 200 °C is typically associated with solvent evaporation and water removal [3]. The significant weight loss between 260 and 462 °C corresponds to the degradation of polymer electrolyte components, particularly PEO-LiTFSI, which undergoes polymer chain breakdown and volatile product release [1,2]. The presence of LSPO within the composite may alter the degradation pathways, potentially stabilizing the polymer matrix and affecting its thermal decomposition profile [4,11]. The plateau phase observed at 462 °C indicates enhanced thermal stability, ensuring that the material can withstand typical battery operating temperatures without significant degradation, thereby improving its durability and performance [10].

The decomposition behavior of the composite electrolyte is crucial for high-temperature battery applications, particularly in electric vehicles and high-power devices where thermal stability is a critical factor [5]. The results demonstrate that integrating LSPO into the polymer matrix enhances the thermal stability of NASICON-PEO composites compared to other ceramic-polymer systems. This highlights the potential of the composite electrolyte for advanced energy storage applications, offering improved durability and performance in demanding operational environments [2,10].

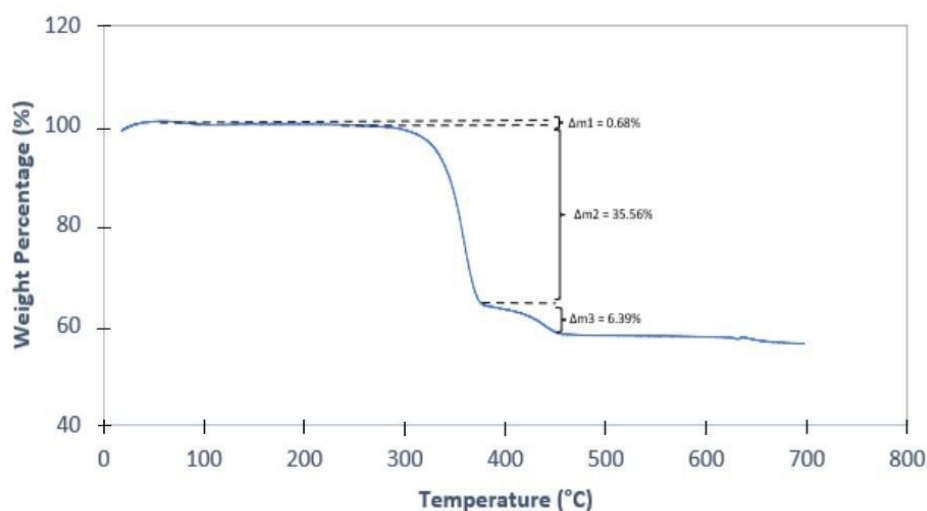


Figure 3 TGA curve of the composite electrolytes sample.

Table 1 Weight loss stages in the composite electrolytes sample.

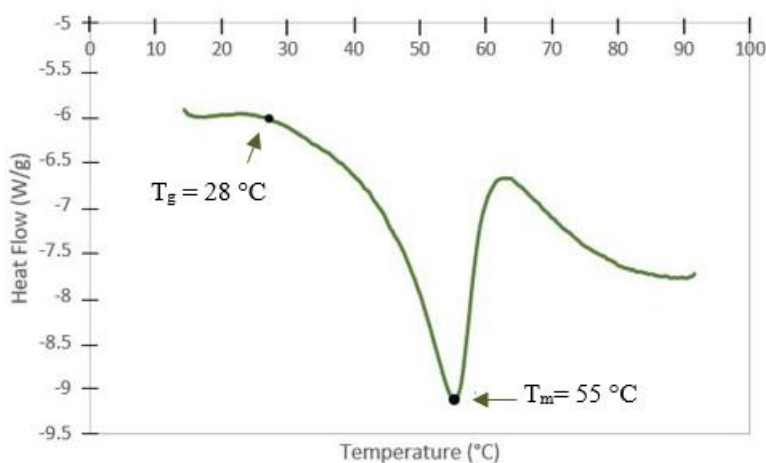
Stage	Temperature range (°C)	Weight loss (%)	Attributed causes
Δm_1	< 200	0.68	Removal of absorbed water and residual solvent [3]
Δm_2	200 - 375	35.56	Decomposition of polymer electrolyte components
Δm_3	375 - 462	6.39	Further degradation of polymer before stabilization

Differential Scanning Calorimetry (DSC) was used to investigate the thermal properties of the composite electrolyte. The DSC curve in **Figure 4** revealed a glass transition temperature (T_g) of 28 °C and a melting temperature (T_m) of 55 °C. The T_g indicates the onset of segmental mobility in the polymer matrix, which is crucial for enhancing ionic conductivity [2,10]. The sharp endothermic peak at T_m signifies a well-defined melting point, suggesting good thermal stability and processability of the material [10,11]. The addition of LSPO ceramic to the polymer electrolyte significantly affects the thermal properties. Higher LSPO content reduces the degree of crystallinity in the polymer matrix, as evidenced by the decrease in the intensity of the endothermic peak and the melting temperature [1,12]. This reduction in crystallinity enhances the flexibility and ionic conductivity of the composite by facilitating ion transport through the polymer-ceramic interfaces [10].

The observed T_g and T_m values have practical implications for the operational temperature range of the composite electrolyte. The material remains stable and functional above T_g , making it suitable for solid-state

battery applications where flexibility and ionic conductivity are critical [2,5]. The thermal stability up to T_m ensures that the composite can withstand typical battery operating temperatures without significant degradation [4,10]. Compared to other polymer-in-ceramic systems, the T_g and T_m values of this composite are competitive. Similar systems often exhibit higher T_g values, which can limit their flexibility and conductivity at lower temperatures [3,12]. The unique combination of thermal stability and reduced crystallinity in this composite enhances its suitability for solid-state batteries, offering improved ionic conductivity and mechanical flexibility [1,10].

The DSC findings are validated by X-ray diffraction (XRD) results, which show reduced crystallinity in the polymer component due to the dispersion of LSPO particles [3,9]. This structural characteristic supports the enhanced ionic conductivity observed in the composite electrolyte, as it facilitates ion transport through both the ceramic and polymer-ceramic interfaces [1,11]. Overall, the thermal properties of this composite electrolyte make it a promising candidate for advanced energy storage applications [2,10].

**Figure 4** DSC graph of composite electrolyte sample.

X-ray diffraction (XRD) analysis of the composite electrolyte provides critical insights into its structural stability and phase composition. **Figure 5** presents the XRD pattern of the composite electrolyte containing 80 wt% LSPO and 20 wt% polymer electrolytes, measured over the 2θ range of 10 to 40°. The observed diffraction pattern aligns well with the standard diffraction data for LSPO, confirming its structural stability within the composite. Notably, the diffraction peaks associated with PEO are not clearly identifiable, which can be attributed to the low X-ray diffraction intensity, suggesting reduced crystallinity in the polymer electrolyte. This reduction is likely due to the dispersion of PEO-LiTFSI within the hot-pressed composite pellet, a phenomenon consistent with previous studies on polymer-ceramic composites [3,7].

The presence of strong LSPO peaks in the composite electrolyte indicates that the integration of LSPO into the polymer matrix does not cause significant structural alterations. Instead, LSPO particles provide a continuous ceramic network, which enhances ionic pathways and mechanical stability which is critical factors for solid-state battery performance [1,10,12]. The reduced crystallinity in PEO benefits the composite by increasing the fraction of amorphous regions, facilitating segmental motion and improving ionic conductivity [2,9]. This structural adjustment aligns with reported findings that amorphous polymer regions contribute to enhanced ion transport and electrode compatibility in polymer-based electrolytes [5,11].

However, the inability to detect PEO peaks in the XRD pattern could also be due to interference from other components or the inherently amorphous nature of the polymer. To validate the dispersion and structural characteristics of PEO within the composite, complementary techniques such as Fourier Transform Infrared Spectroscopy (FTIR) or Raman spectroscopy could provide additional insights [7]. FTIR analysis could confirm the molecular interactions between PEO and LSPO by identifying characteristic functional group shifts, while Raman spectroscopy could help detect vibrational modes specific to PEO that may be indistinguishable in XRD [7]. Future studies incorporating these techniques would offer a more comprehensive understanding of the structural properties of the composite electrolyte.

Compared to other NASICON-PEO systems, the sharp and intense peaks in the XRD pattern suggest a well-defined LSPO structure, distinguishing it from systems where peak broadening occurs due to poor ceramic dispersion [3,9]. Overall, the structural stability of the composite, as demonstrated by the XRD results, supports its potential for use in solid-state battery applications. The integration of LSPO into the polymer matrix preserves the crystalline framework while simultaneously reducing polymer crystallinity, enhancing ion transport, and maintaining mechanical robustness which is the key attributes for high-performance energy storage devices [5,10].

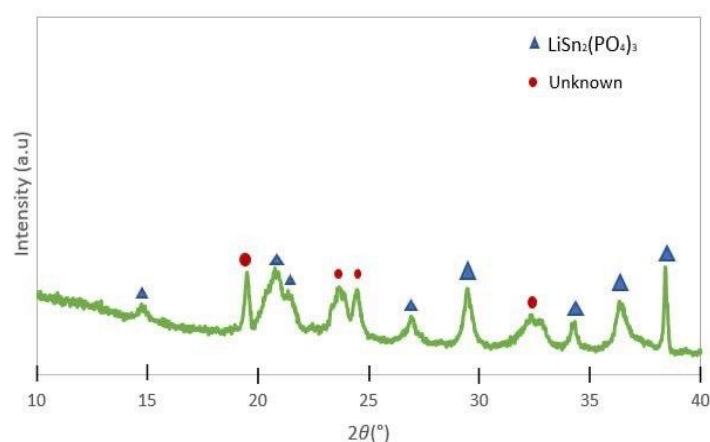


Figure 5 X-ray diffraction pattern of the composite electrolytes sample.

Electrochemical Impedance Spectroscopy (EIS) was employed to investigate the electrical properties of

the composite sample. The complex impedance plots of the composite sample at various temperatures (30, 40,

50, 60, 70, 80 and 90 °C) are presented in **Figures 6(a) - 6(d)**. The Nyquist plots typically consist of a semicircle in the high-frequency region, representing the bulk response, and an electrode spike in the low-frequency region. The intersection of the semicircle with the x-axis corresponds to the bulk resistance (R_b), which directly influences ionic conductivity [9].

The spike observed at low frequencies in the impedance plot is indicative of electrode polarization, which arises due to ion accumulation at the electrode-electrolyte interface and interfacial resistance. This phenomenon occurs when migrating ions build up at the interface instead of freely diffusing, leading to a deviation from ideal ionic conduction behavior [15] particularly evident at 50 and 60 °C. High interfacial resistance can further exacerbate polarization by impeding charge transfer, which negatively affects overall electrolyte performance [16]. To minimize electrode polarization, several strategies can be employed such as enhancing electrode-electrolyte compatibility by using surface-modified electrodes or interfacial buffer layers can facilitate better ion exchange and reduce accumulation effects [17]. Additionally, reducing interfacial resistance through the incorporation of conductive additives or optimizing the polymer-ceramic interface can promote seamless ion migration, improving overall conductivity [18]. By

addressing these factors, the composite electrolyte can achieve more stable and efficient charge transport, making it a stronger candidate for solid-state battery applications.

The temperature-dependent behavior of ionic conductivity is primarily influenced by segmental motion in the polymer matrix and ion transport pathways in the LSPO ceramic [15]. As temperature increases, polymer chains gain mobility, facilitating ion hopping and enhancing conductivity [16]. The conductivity reaches an optimal value of 6.2825×10^{-5} S/cm at 50 °C, suggesting that ion mobility is maximized due to the combined effect of polymer relaxation and ceramic-assisted pathways [17]. Beyond 50 °C, the conductivity decline may be attributed to thermal instability or a loss of interfacial contact between LSPO and the polymer matrix [18]. Excessive polymer segmental motion can disrupt the ion coordination environment, reducing the efficiency of ion transport [19]. Additionally, at higher temperatures, phase separation or increased polymer softening may create discontinuities in ionic pathways, leading to higher resistance [20]. These findings highlight the importance of optimizing the polymer-ceramic interface to maintain stable conductivity across a broad temperature range.

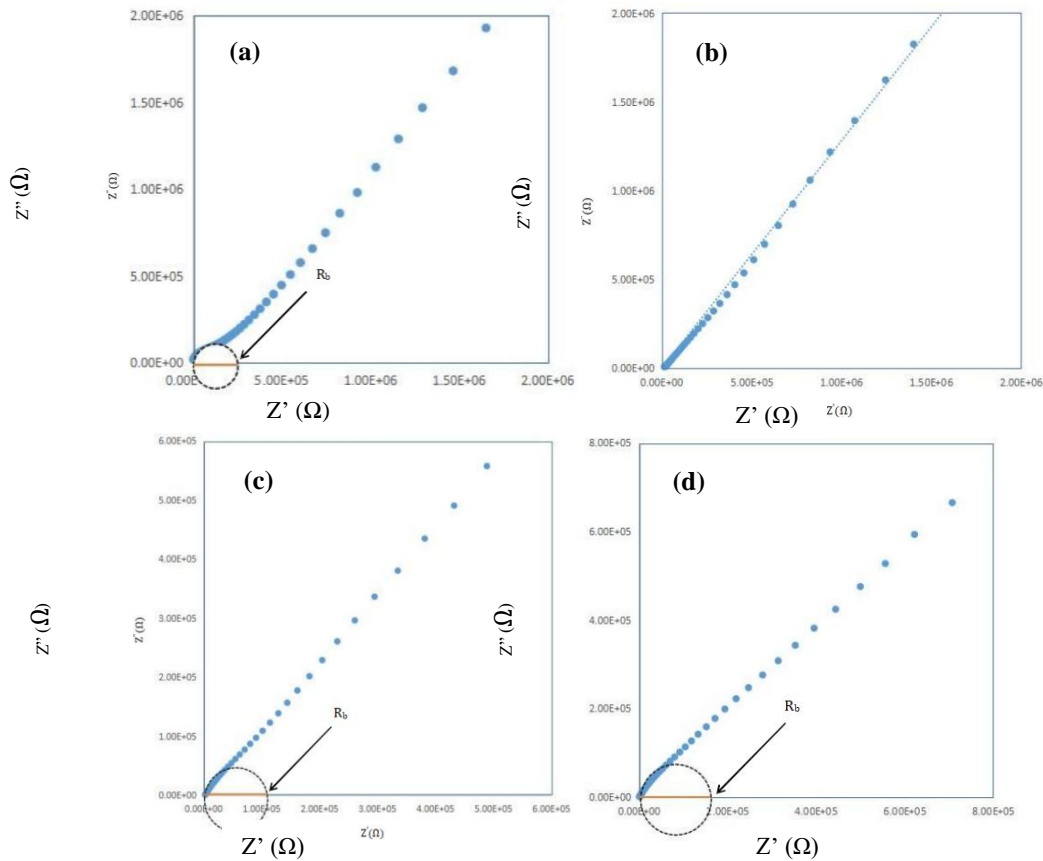


Figure 6 Impedance plot of the composite sample at (a) 30 °C, (b) 50 °C, (c) 70 °C, and (d) 90 °C.

The ionic conductivity of the samples at different temperatures is summarized in **Table 2**. The bulk resistance (R_b) initially increases from 30 to 50 °C and subsequently decreases from 60 to 90 °C. Correspondingly, the bulk conductivity (σ_b) rises with temperature up to 50 °C, reaching an optimal value of 6.2825×10^{-5} S/cm. This trend can be attributed to enhanced segmental motion in the polymer matrix and improved ion transport pathways within the LSPO ceramic phase [6]. However, beyond 50 °C, the rate of conductivity increase slows down, possibly due to thermal instability or a loss of interfacial contact between the ceramic and polymer components [4].

Beyond 50 °C, the conductivity decline may be attributed to thermal instability or a loss of interfacial contact between LSPO and the polymer matrix. Excessive polymer segmental motion can disrupt the ion coordination environment, reducing the efficiency of ion transport. Additionally, at higher temperatures, phase separation or increased polymer softening may create discontinuities in ionic pathways, leading to higher resistance. These findings highlight the importance of optimizing the polymer-ceramic interface to maintain stable conductivity across a broad temperature range.

Table 2 The R_b and σ_b of composite samples at different temperatures.

Temperature (°C)	R_b (Ω)	σ_b (Scm^{-1})
30	2.8467×10^5	5.2693×10^{-6}
40	2.3876×10^4	5.8464×10^{-6}
50	2.3876×10^4	6.2825×10^{-5}
60	3.5351×10^4	4.2432×10^{-5}
70	5.9682×10^5	2.5133×10^{-6}

Temperature (°C)	R_b (Ω)	σ_b (Scm^{-1})
80	4.1701×10^5	3.5970×10^{-6}
90	4.8226×10^5	3.1104×10^{-6}

The optimal ionic conductivity at 50 °C aligns well with typical operating temperatures of solid-state batteries and surpasses many reported composite electrolytes. Specifically, the conductivity of 6.2825×10^{-5} S/cm at 50 °C is significantly higher than that of PEO-LiTFSI systems, as shown in **Table 3** [3]. This superior performance can be attributed to the high ceramic content (80 wt% LSPO) and the optimized polymer-ceramic interface, which facilitates efficient ion transport [2]. Since a decrease in R_b directly improves conductivity, the structural uniformity of the LSPO-polymer matrix plays a crucial role in reducing resistance and enhancing overall ionic transport [8].

Compared to industry benchmarks, the observed conductivity surpasses many conventional PEO-based electrolytes and approaches the performance of high-conductivity polymer-ceramic composites [1,3]. This enhancement is primarily due to the high ceramic content (80 wt% LSPO) and the optimized polymer-ceramic interface, which facilitate rapid ion migration. Improved conductivity directly impacts battery performance by enabling higher charge/discharge rates, increased energy density, and better cyclability, making it viable for applications requiring high power output

and long cycle life. By ensuring stable conductivity at relevant temperatures, this composite electrolyte contributes to the advancement of solid-state lithium batteries, offering a safer and more efficient alternative to liquid electrolytes. Further optimization of the polymer-ceramic interface could enhance its performance, bringing it closer to commercial adoption. In summary, the composite electrolyte demonstrates promising electrical properties, with optimal ionic conductivity at 50 °C. This finding has significant implications for solid-state battery applications, as it suggests improvements in energy storage efficiency and safety. Further optimization of the polymer-ceramic interface and reduction of electrode polarization could enhance the practical applicability of this composite electrolyte system [1,5]. The optimal ionic conductivity of 6.2825×10^{-5} S/cm at 50 °C aligns well with typical solid-state battery operating temperatures, making this composite electrolyte a strong candidate for next-generation energy storage. This temperature range ensures efficient ion transport while maintaining thermal stability, which is crucial for improving battery safety and longevity.

Table 3 Comparison of ionic conductivity of various composite electrolytes.

Composite	Conductivity (S/cm)	Temperature (°C)	Performance remarks	Ref.
P(PEO-LiTFSI) - 20 wt % LSPO - 80 wt %	6.2825×10^{-5}	50	High conductivity due to high ceramic content (80 wt% LSPO), enhanced polymer-ceramic interface, and improved ion transport pathways.	This work
P(CL-TMC) - 80 wt % LLZO (28 wt % LiTFSI) PEO - 80 wt %	1.4×10^{-5}	30	Lower conductivity due to insufficient polymer-ion interaction.	[3]
LLZTO - 5 wt % PEG (PEO-LiTFSI 8:1)	1.5×10^{-5}	25	Improved conductivity via PEG plasticization, but lower than this work due to limited ceramic content.	[10]
PCL - 75 wt % LAGP (30 wt.% LiTFSI)	1.14×10^{-5}	30	Moderate conductivity, but lacks optimized ion pathways.	[11]

Composite	Conductivity (S/cm)	Temperature (°C)	Performance remarks	Ref.
PEO - 82.5 wt % LLZO (PEO-LiTFSI 15:1)	1.3×10^{-4}	60	Higher conductivity at 60 °C, but not directly comparable at 50 °C.	[12]
PB/A - 80 wt % LAGP (PBA-LiClO ₄ 6:1)	8×10^{-7}	25	Very low conductivity due to poor ion transport in the polymer matrix.	[13]
PEO - 80 wt % LICGC (PEO-LiTF 16:1)	1×10^{-6}	30	Low ionic conductivity due to weaker ion dissociation.	[14]

Conclusions

In this study, a composite electrolyte consisting of 80 wt% LSPO (Lithium Superionic Conductors) and 20 wt% polyethylene oxide (PEO) with LiTFSI salt was successfully prepared using the solution casting method. Thermogravimetric analysis (TGA) revealed gradual weight loss, primarily attributed to the decomposition of the PEO components within the composite. The incorporation of PEO into LSPO significantly enhanced the thermal stability of the composite electrolyte. Differential scanning calorimetry (DSC) results showed that the glass transition temperature (T_g) of the composite electrolyte was 28 °C, while the melting temperature (T_m) was 55 °C. X-ray diffraction (XRD) measurements confirmed the crystallinity of the composite, showing a decrease in XRD intensity with a reduction in crystallinity. Notably, the diffraction peaks corresponding to PEO were not observed in the XRD pattern, likely due to the low X-ray diffraction from the semi-crystalline nature of the polymer. Electrochemical Impedance Spectroscopy (EIS) measurements were conducted at various temperatures (30, 40, 50, 60, 70, 80 and 90 °C) to determine the bulk conductivity. The results showed that the addition of 20 wt% polymer electrolyte into the ceramic matrix enhanced the conductivity, with the highest value of 6.2825×10^{-5} S/cm observed at 50 °C. In conclusion, the NASICON/PEO polymer-in-ceramic composite electrolyte exhibited improved thermal, structural, and electrical properties, making it a promising candidate for use in solid-state batteries.

Acknowledgements

The authors gratefully acknowledge the assistance and lab facilities provided by the Faculty of Applied Sciences, Universiti Teknologi MARA, Malaysia, Centre of Foundation Studies, Universiti Teknologi MARA, Malaysia and International Battery Center (IBC) Sdn. Bhd, Malaysia.

References

- [1] SA Ahmed, T Pareek, S Dwivedi, M Badole and S Kumar. Polymer-in-ceramic composite electrolyte with high ionic conductivity for all-solid-state lithium batteries. *Journal of Solid-State Electrochemistry* 2020; **24**, 2407-2417.
- [2] P Yao, H Yu, Z Ding, Y Liu, J Lu, M Lavorgna, J Wu and X Liu. Review on polymer-based composite electrolytes for lithium batteries. *Frontiers in Chemistry* 2019; **7**, 522.
- [3] FP Nkosi, M Valvo, J Mindemark, NA Dzulkurnain, G Hernández, A Mahun, S Abbrent, J Brus, L Kobera and K Edström. Garnet-poly(ϵ -caprolactone-co-trimethylene carbonate) polymer-in-ceramic composite electrolyte for all-solid-state lithium-ion batteries. *ACS Applied Energy Materials* 2021; **4**(3), 2531-2542.
- [4] Z Wei, Y Ren, M Wang, J He, W Huo and H Tang. Improving the conductivity of solid polymer electrolyte by grain reforming. *Nanoscale Research Letters* 2020; **15**, 122.
- [5] Y Chen, Y Kang, Y Zhao, L Wang, J Liu, Y Li, Z Liang, X He, X Li, N Tavajohi and B Li. A review of lithium-ion battery safety concerns: The issues,

- strategies, and testing standards. *Journal of Energy Chemistry* 2020; **59**, 83-99.
- [6] J Zhang, B Li, Q Wang, X Wei, W Feng, Y Chen, P Huang and Z Wang. Application of fourier transform infrared spectroscopy with chemometrics on postmortem interval estimation based on pericardial fluids. *Scientific Reports* 2017; **7(1)**, 18013.
- [7] A Nandiyanto, R Oktiani and R Ragadhita. How to read and interpret FTIR spectroscopy of organic material. *Indonesian Journal of Science and Technology* 2019; **4(1)**, 97-118.
- [8] AK Manohar, O Bretschger, KH Nealson and F Mansfeld. The use of electrochemical impedance spectroscopy (EIS) in the evaluation of the electrochemical properties of a microbial fuel cell. *Bioelectrochemistry* 2008; **72(2)**, 149-154.
- [9] NA Mustafa, S Adnan, M Sulaiman and NS Mohamed. Low-temperature sintering effects on NASICON-structured solid electrolytes prepared via citric acid-assisted sol-gel method. *Ionic* 2015; **21**, 955-965.
- [10] L Chen, Y Li, SP Li, LZ Fan, CW Nan and JB Goodenough. PEO/garnet composite electrolytes for solid-state lithium batteries: From “ceramic-in-polymer” to “polymer-in-ceramic”. *Nano Energy* 2018; **46**, 176-184.
- [11] B Zhang, Y Liu, J Liu, L Sun, L Cong, F Fu, A Mauger, CM Julien, H Xie and X Pan. Polymer-in-ceramic based poly(ϵ -caprolactone)/ceramic composite electrolyte for all-solid-state batteries. *Journal of Energy Chemistry* 2021; **52**, 318-325.
- [12] JH Choi, CH Lee, JH Yu, CH Doh and SM Lee. Enhancement of ionic conductivity of composite membranes for all-solid-state lithium rechargeable batteries incorporating tetragonal LLZO into a polyethylene oxide matrix. *Journal of Power Sources* 2015; **274**, 458-463.
- [13] MS Park, YC Jung and DW Kim. Hybrid solid electrolytes composed of poly(1,4-butylene adipate) and lithium aluminum germanium phosphate for all-solid-state Li/Li cells. *Solid State Ionics* 2018; **315**, 65-70.
- [14] AS Pandian, XC Chen, J Chen, BS Lokitz, RE Ruther, G Yang, K Lou, J Nanda, FM Delnick and NJ Dudney. Facile and scalable fabrication of polymer-ceramic composite electrolyte with high ceramic loadings. *Journal of Power Sources* 2018; **390**, 153-164.
- [15] RC Agrawal and GP Pandey. Solid polymer electrolytes: Materials designing and all-solid-state battery applications. *Journal of Physics D: Applied Physics* 2008; **41(22)**, 223001.
- [16] PG Bruce, B Scrosati and JM Tarascon. Nanomaterials for rechargeable lithium batteries. *Angewandte Chemie International Edition* 2008; **47(16)**, 2930-2946.
- [17] B Kumar and LG Scanlon. Polymer-ceramic composite electrolytes. *Journal of Power Sources* 1994; **52(2)**, 261-268.
- [18] D Zhou, D Shanmukaraj, A Tkacheva, M Armand and G Wang. Polymer electrolytes for lithium-based batteries: Advances and prospects. *Chem* 2019; **5(9)**, 2326-2352.
- [19] JR MacCallum and CA Vincent. *Polymer electrolyte reviews*. Elsevier Applied Science, London, 1987.
- [20] V Aravindan, J Gnanaraj, S Madhavi and HK Liu. Lithium-ion conducting electrolyte salts for lithium batteries. *Chemistry - A European Journal* 2011; **17(51)**, 14326-14346.